ARTICLE
Journal of Cellular Biochemistry 111:1125–1137 (2010)

Journal of Cellular Biochemistry

Recycling and LFA-1-Dependent Trafficking of ICAM-1 to the Immunological Synapse

Jae-Hyeok Jo, Min-Sung Kwon, Hyang-Ok Choi, Hyun-Mee Oh, Hyang-Jin Kim, and Chang-Duk Jun*

School of Life Sciences, Cell Dynamics Research Center, BioImaging Research Center, and Immune Synapse Research Center, Gwangju Institute of Science and Technology, Gwangju 500-712, Republic of Korea

ABSTRACT

Little is known about how adhesion molecules on APCs accumulate at immunological synapses. We show here that ICAM-1 on APCs is continuously internalized and rapidly recycled back to the interface after antigen-priming T-cell contact. The internalization rate is high in APCs, including Raji B cells and dendritic cells, but low in endothelial cells. Internalization is significantly reduced by inhibitors of Na^+/H^+ exchangers (NHEs), suggesting that members of the NHE-family regulate this process. Once internalized, ICAM-1 is co-localized with MHC class II in the polarized recycling compartment. Surprisingly, not only ICAM-1, but also MHC class II, is targeted to the immunological synapse through LFA-1-dependent adhesion. Cytosolic ICAM-1 is highly mobile and forms a tubular structure. Inhibitors of microtubule or actin polymerization can reduce ICAM-1 mobility, and thereby block accumulation at immunological synapses. Membrane ICAM-1 also moves to the T-cell contact zone, presumably through an active, cytoskeleton-dependent mechanism. Collectively, these results demonstrate that ICAM-1 can be transported to the immunological synapse through the recycling compartment. Furthermore, the high-affinity state of LFA-1 on T cells is critical to induce targeted movements of both ICAM-1 and MHC class II to the immunological synapse on APCs. J. Cell. Biochem. 111: 1125–1137, 2010.

KEY WORDS: ICAM-1; LFA-1; MHC CLASS II; IMMUNOLOGICAL SYNAPSE; POLARIZED RECYCLING COMPARTMENT

Binding of the TCR to peptides presented on MHC molecules is the key event driving T-cell development and activation. In general, this event is achieved by a dynamic spatial molecular architecture, termed the immunological synapse, between T cells and APCs [Monks et al., 1998; Grakoui et al., 1999]. The immunological synapse consists of a central supramolecular activation cluster (cSMAC) that is highly enriched for TCRs and the associated peptide-MHC (pMHC) complex. The cSMAC is surrounded by a peripheral SMAC (pSMAC) consisting of LFA-1 and ICAM-1 adhesion proteins [Monks et al., 1998; Grakoui et al., 1999].

The mechanisms by which T-cell SMAC molecules transport to the immunological synapse have been the subject of extensive investigation [Das et al., 2004; Cairo et al., 2006; Kaizuka et al., 2007; Nolz et al., 2007]. TCR accumulation at the immunological synapse is controlled by T-cell polarity, TCR endocytosis and recycling, and vesicle fusion mediated by SNARE complexes [Das et al., 2004]. Rab35 and RabGAP are known to regulate TCR recycling and immunological synapse formation [Patino-Lopez et al., 2008]. Based on the planar lipid bilayer model, an actin-based continual transport of TCR to the center has also been proposed to explain the formation of the cSMAC and sustained T-cell signaling [Campi et al., 2005; Yokosuka et al., 2005; Varma et al., 2006]. Cytoskeletal regulation also couples to the lateral motility of integrins, leading to LFA-1 conformational changes and clustering at the cell periphery during SMAC formation [Cairo et al., 2006; Kaizuka et al., 2007]. WAVE2-ARP2/3-mediated de novo actin polymerization has been reported to induce integrin clustering and high-affinity binding through the recruitment of vinculin and talin [Nolz et al., 2007]. Membrane and/or intracellular trafficking of other SMAC molecules, including CD28, CTLA-4, and CD38, also have been studied in T cells [Egen and Allison, 2002; Taner et al., 2004; Munoz et al., 2008; Gorska et al., 2009]. Distinct signals control trafficking of intracellular and cell-surface proteins to the immunological synapse. For instance, ZAP-70 controls the

Jae-Hyeok Jo and Min-Sung Kwon contributed equally to this work.

Additional Supporting Information may be found in the online version of this article.

Grant sponsor: MEST/KOSEF; Grant numbers: R01-2008-000-20989-0, R11-2007-007-01002-0, 2008-C00265; Grant sponsor: BioImaging Research Center in GIST.

*Correspondence to: Prof. Dr. Chang-Duk Jun, School of Life Sciences, GIST, Gwangju 500-712, Republic of Korea. E-mail: cdjun@gist.ac.kr

Received 26 January 2010; Accepted 21 July 2010 • DOI 10.1002/jcb.22798 • © 2010 Wiley-Liss, Inc.
Published online 2 August 2010 in Wiley Online Library (wileyonlinelibrary.com).

re-orientation of the microtubule organizing center (MTOC), and the translocation of intracellular CD3ζ, linker for activation of T cells (LAT), and PKCθ to the immunological synapse [Blanchard et al., 2002].

In contrast to the T-cell segment of the immunological synapse, little is known about how APC SMAC molecules are transported to the immunological synapse and organized into the each subarea of SMACs. It has been reported that MHC class II molecules are highly enriched in tubular endosomes of matured dendritic cells (DCs) [Boes et al., 2002; Chow et al., 2002]. This specialized tubule from lysosomal compartments extends intracellularly and fuses directly with the plasma membrane [Boes et al., 2002; Chow et al., 2002]. A recent report demonstrated that the peptide-loaded MHC complexes are internalized and recycled by tubules containing Arf6 and Rab35, which are small GTPases that are thought to be involved in clathrin-independent protein sorting [Walseng et al., 2008]. In contrast to MHC class II molecules, whose internalization, sorting, and trafficking to the cell surface is heavily dependent on the cell's maturation status and the antigen peptides, the pathways of other SMAC molecules, including ICAM-1, have not been explored in depth. With respect to this underlying question, we examined the trafficking and accumulation mechanisms of ICAM-1, an important pSMAC molecule on APCs, to the immunological synapse during T-cell contact. Moreover, it is poorly understood whether accumulation of SMAC molecules in APCs is solely a passive mechanism triggered by contact with an antigen-recognizing T cell or if it requires a cytoskeleton-mediated activation mechanism.

ICAM-1 is a type I membrane protein and a ligand for at least two integrins, LFA-1 (CD11a/CD18) and Mac-1 (CD11b/CD18), on leukocytes [Springer, 1990, 1994]. ICAM-1, by interacting with LFA-1, plays a core role in forming an immunological synapse at T cell–APC contact sites, thereby enhancing immune responses [Monks et al., 1998; Grakoui et al., 1999]. Nevertheless, little is known about how ICAM-1 transportation to and accumulation at the immunological synapse occurs. Several routes can be envisaged, either on the cell surface or through the cell interior. In the current study, we found that ICAM-1 is continuously internalized on APCs and rapidly recycled back to the interface of T cell–APC contact. This finding is in contrast to previous work on endothelial cells [Muro et al., 2003, 2005, 2006]. We found that internalized ICAM-1 is co-localized with MHC class II by accumulation in the polarized recycling compartment of APCs. Upon contact with antigen-recognizing T cells, trafficking of these two SMAC molecules to the immunological synapse was controlled by high-affinity LFA-1 and was dependent on actin and microtubules. We found that membrane ICAM-1 (mIC1) also moves to the T-cell contact zone, potentially through an active transport mechanism mediated by the cytoplasmic domain and the actin cytoskeleton.

MATERIALS AND METHODS

REAGENTS AND ANTIBODIES

LPS, colchicine (COL), cytochalasin B (CB), brefeldin A, monodancyl cadaverine (MDC), filipin, amiloride (AMR), 5-(*N*-ethyl-*N*-isopropyl)amiloride (EIPA), phorbol 12-myristate 13-acetate (PMA), staurosporine, rottlerin, and latruculin A were obtained from Sigma (St. Louis, MO). Tubulin tracker (Oregon Green 488 Taxol, bis-acetate) and green fluorescent cell tracker CMFDA were obtained from Molecular Probes (Eugene, OR). Staphylococcal enterotoxin E (SEE) and staphylococcal enterotoxin B (SEB) were obtained from Toxin Technology (Sarasota, FL). Recombinant human GM-CSF and IL-4 were obtained from PeproTech Inc. (Princeton, NJ).

Antibodies to human ICAM-1 (R6.5, CA-7 and CBR IC1/11) and LFA-1 (CBR-LFA-1/2, TS2/4, and TS1/22) were purified from hybridoma supernatants using an Affi-Gel Protein A MAPS kit (Bio-Rad, Hercules, CA) according to the manufacturer's instructions. Anti-ICAM-1 (CBR IC1/11) Fab was prepared by papain cleavage using an ImmunoPure Fab Preparation kit (Pierce, Rockford, IL) according to the manufacturer's instructions. Anti-human HLA-DR (MHC class II)-PE-cy5.5 antibody was acquired from Invitrogen (Eugene, OR). Mouse anti-human transferrin receptor (TfR) antibody was obtained from Zymed (San Francisco, CA). FITC-conjugated goat anti-mouse IgG was purchased from Sigma. Conjugation of anti-ICAM-1 and anti-LFA-1 mAbs (including Fab) to cy3, cy5, or Alexa 488 bisfunctional dyes (Pierce, Rockford, IL) were performed according to the manufacturer's instructions. Anti-Alexa Fluor 488 rabbit IgG was obtained from Molecular Probes.

CELL CULTURES

Human Jurkat T JE6.1 (TIB-152, ATCC) and Raji B (CCL-86, ATCC) cell lines were grown in RPMI-1640 medium supplemented with 10% FBS, 100 IU/ml penicillin G, 100 μg/ml streptomycin, and 2 mM L-glutamine. HUVEC cells were isolated from two to five umbilical cord veins, pooled, and established as primary cultures in a complete endothelial growth medium (EGM; Cambrex Bioscience Inc., Rockland, ME) supplemented with 2% FBS, bovine brain extract (BBE), hEGF, hydrocortisone, and gentamycin, according to the manufacturer's instructions.

IN VITRO GENERATION OF DCs

Human peripheral blood mononuclear cells were isolated from normal donors by dextran-sedimentation followed by centrifugation through a discontinuous Ficoll gradient (Amersham Biosciences, Little Chalfont, England). Sixty millimeters of culture dishes were seeded with 2×10^7 cells and incubated for 6 h in a humidified chamber at 37°C and 5% CO_2. After removing non-adherent cells, remaining adherent cells were supplied with 5 ml fresh complete RPMI-1640 medium containing 50 ng/ml GM-CSF and 10 ng/ml IL-4 to induce DC differentiation. After 6 days of incubation at 37°C, DCs were incubated with 1 μg/ml LPS for 18 h to induce maturation. Culture medium containing these cytokines was replaced every 3 days.

cDNA TRANSFECTION

Human wild-type ICAM-1 cDNA (wt-IC1_GFP) (19) and ICAM-1 lacking the cytoplasmic domain (IC1ΔCTD_GFP) (19) were prepared as described previously. Raji B cells were transiently transfected with ICAM-1 cDNAs using the Nucleofector Kit V (Amaxa, Koeln, Germany), following the manufacturer's guidelines. After 24–48 h of transfection, cells were used for the T cell–APC conjugate assay and FRAP analysis.

SEB-ACTIVATED PBLTs

Polyclonal SEB-activated PBL-derived T cells (S-PBLT cells) were generated by incubating PBLs with peripheral blood monocytes in medium supplemented with 0.5 μg/ml SEB and 50 U/ml IL-2. Cells were restimulated every 3 days for subsequent SEB-specific T-cell proliferation.

T CELL–APC CONJUGATE FORMATION

Jurkat T cells were stained with CMFDA (Molecular Probes) for 30 min. Raji B cells (1×10^5 cells/well) pre-treated with various reagents were incubated with 5 μg/ml SEE (or vehicle control) for the indicated times. In some cases, CBR-LFA-1/2 mAb (activating antibody) was used instead of SEE to directly activate LFA-1 on T cells. TS-1/22 was used to block the LFA-1-ICAM-1 interaction. For conjugate formation between DCs and S-PBLTs, 0.5 μg/ml SEB was loaded onto DCs. ICAM-1 accumulation at the T cell–APC contact site was calculated as a ratio of fluorescence intensity at the contact region (F_{con}) to the fluorescence intensity at the opposite site (F_{oppo}). The data were obtained, processed, and analyzed by Olympus FLUOVIEW software version 2.0 (Olympus Corporation, Tokyo, Japan).

In some case, translocation of receptors or MTOC was expressed as the percentage of conjugates with MTOC, ICAM-1, or MHC class II clusters redistributed close to the T cell–APC contact area. Over 50 conjugates were analyzed by random selection from at least three independent experiments.

CONFOCAL AND LIVE-CELL IMAGING ANALYSIS

Live-cell and time-lapse imaging was performed using an FV1000 confocal laser scanning microscope (Olympus Corporation, Tokyo, Japan) equipped with a live-cell chamber device (Live Cell Instrument Inc., Seoul, Korea). During live-cell imaging, chamber devices were maintained at 37°C in a 5% CO_2 atmosphere. The confocal series of fluorescence and differential interference contrast (DIC) images were simultaneously obtained at different time intervals using 60–100× oil immersion objectives on the FV1000 confocal microscope. The images were processed and assembled into videos using Olympus FLUOVIEW software version 2.0 and Metamorpho offline version 7.6.0.0 (Molecular Devices, Downingtown, PA). Trafficking distance and speed was calculated from the total length of the trafficking path during a 60-s period by Metamorpho offline.

For the co-localization analyses, the Z section cutting area through the apical surface was chosen. Images captured at different wavelengths were superimposed and the intensity of expression for each fluorochrome in the field was then plotted in a scattergram using FLUOVIEW software. The overlapping degree of intensity (ODI) values were calculated using FLUOVIEW software. The co-localization percentage was calculated as the ODI multiplied by 100.

INTERNALIZATION ANALYSIS

For receptor internalization experiments, 1×10^5 Raji B cells were treated with cy3-, cy5-, or Alexa 488-conjugated mouse monoclonal ICAM-1 antibodies (10 μg/ml CBR IC1/11 Fab or IgG) or 10 μg/ml anti-HLA-DR-PE-cy5.5 mAb for 1 h at 4°C and then returned to a 37°C incubator. At the indicated time points, the samples were washed and mounted onto the live chamber. For the staining of internalized TfRs and the co-localization analysis with ICAM-1, cells were stained with anti-IC1-cy3 IgG for 2 h at 37°C. The cells were then fixed with 4% paraformaldehyde, permeabilized for 20 min with 0.1% saponin in PBS, washed, and incubated for 2 h at 37°C with mouse anti-human TfR antibody, followed by a FITC-conjugated secondary antibody. The co-localization study of ICAM-1 with MTOC was conducted by simultaneously staining both ICAM-1 (anti-IC1-cy3 IgG) and MTOC (tubulin tracker, 250 nM) at 4°C for 1 h and then at 37°C for 3 h. Receptor internalization was quantified by the fluorescence (F) ratio of cytoplasmic ICAM-1 (F_{cyto}) to mIC1 (F_{mem}): F ratio $= F_{cyto}/F_{mem}$; Note, $F_{cyto} = F_{whole} - F_{mem}$ in the single cell.

Receptor internalization was also measured by flow cytometry using a FACScan cell analyzer (Becton Dickinson, San Jose, CA). Briefly, Raji B cells were stained with anti-IC1-Alexa 488 IgG for 1 h at 4°C. The cells were treated with the reagents indicated in the text and further incubated for 30 min at 37°C. The external membrane antibodies (anti-IC1-Alexa 488 IgG) were quenched by anti-Alexa 488-rabbit IgG for 1 h at 4°C. The rate of internalization was quantified by mean fluorescence intensity (MFI) for each experiment. Negative and positive controls included non-stained or stained cells without quenching, respectively.

LABELING OF MEMBRANE AND CYTOSOLIC ICAM-1

To label internalized cytosolic ICAM-1 (cIC1), the objective cells (1×10^5 Raji B, DC, or HUVEC) were treated with 10 μg/ml anti-IC1-cy5 IgG for 2 h at 37°C. For Raji B cells, the external antibodies were acid washed with complete pH 2.0 RPMI-1640 medium for 1 min and immediately neutralized with an equal volume of pH 12.0 medium. For staining of mIC1, after washing, the cells were re-stained with anti-IC1-cy3 Fab (10 μg/ml) for 1 h at 4°C. The acid washing step was eliminated for DCs and HUVECs.

FRAP ANALYSIS

Raji B cells were transiently transfected for 24 h with wt-IC1_GFP or IC1ΔCTD_GFP [Oh et al., 2007]. The cells were viewed on poly-L-lysine-coated coverslips mounted in a chamber device using RPMI 1640 without phenol red supplemented with 5% FBS and 25 mM HEPES. FRAP experiments were carried out on a FV1000 confocal laser scanning microscope (Olympus Corporation) using a 100× objective at 37°C. Transiently transfected cells expressing intermediate levels of GFP were chosen for FRAP analysis, allowing the use of similar microscope settings for all experiments. A selected area (2-μm square) of the IC1_GFP on the cell membrane was photobleached for 3–5 s by 488-nm laser at 18 mW. Pre- and post-bleach images were collected periodically until fluorescence was recovered at a plateau level, at which point the fluorescence intensity in the photo-bleached area of each image was measured. The post-bleach intensity was corrected for overall loss of fluorescence determined from total fluorescence in the whole-cell images taken at the beginning and end of the experiment. The mobile fraction was calculated according to $M_F = (F_\infty - F_0)/(F_i - F_0)$ where F_∞ is the average fluorescence after full recovery, F_0 is the fluorescence immediately following photo-bleaching, and F is the average fluorescence before photo-bleaching. The half-time of

recovery t was calculated by fitting the recovery curve to the empirical equation $F(t) = F_0 + ((F_\infty - F_0) \times t)/(t + t_{1/2})$.

STATISTICS

Mean values were calculated from data taken from at least three or more separate experiments conducted on separate days. Where significance testing was performed, unpaired Student's t-tests and one-way ANOVA tests were used. We considered differences between groups as significant at $P < 0.05$.

ONLINE SUPPLEMENTAL MATERIALS

Video 1 (corresponding to Fig. 1) shows polarization and trafficking of internalized ICAM-1 to the T cell–APC contact zone. Video 2A (corresponding to Fig. 8B) demonstrates dynamic and bidirectional movement of internalized ICAM-1 in primary human DCs. Videos 2B and C show the effects of COL and CB on internalized ICAM-1 movement in primary human DCs.

RESULTS

T-CELL CONTACT WITH APCs INDUCED THE POLARIZATION OF ICAM-1 RECYCLING TO THE T CELL–APC CONTACT ZONE

During the immunological synapse study, we unexpectedly found that mIC1 was easily internalized into the cytosolic compartments of B cells where they formed a large cluster (Figs. 1 and 2A). After T cell–APC contact in the presence of the superantigen SEE, the large ICAM-1 cluster in the APC became oriented toward the T-cell contact point (Fig. 1 and Supplementary Video 1). The large ICAM-1 cluster was identified as a polarized endosomal recycling compartment similar to those for recycling TCRs [Das et al., 2004]. Further, small ICAM-1 clusters became separated from the large polarized cluster and continuously traveled to the T-cell contact, which correlated with a proportional decrease in cIC1 (Fig. 1 and Supplementary Video 1). Approximately 70% of the T cell–APC conjugates formed in the presence of superantigen showed accumulation of ICAM-1 clusters in the contact zone versus only 16% in control cells (Fig. 1A). Interestingly, time-lapse confocal microscopic analysis revealed that delayed-sequential binding of two Jurkat T cells to one Raji B cell induced separation of ICAM-1 clusters to both sides (Fig. 1B), suggesting that internalized ICAM-1 can transport to immunological synapses in APCs. This result further suggests that, in contrast to previous reports [Kupfer et al., 1986; Kuhne et al., 2003], asymmetrical polarization significantly occurred in APCs during interaction with T cells. Overall, these findings led to further investigation of the pathways and mechanisms of ICAM-1 transport to the immunological synapse.

It has been reported that internalization of ICAM-1 requires multimeric forms because monomeric (Fab) anti-ICAM-1 antibody does not significantly trigger internalization of ICAM-1 in endothelial cells [Muro et al., 2003]. However, there was no difference in the levels of internalization of ICAM-1 in Raji B cells treated with monomeric anti-ICAM-1 antibody (Fab fragment of CBR-IC1/11 conjugated with cy3, anti-IC1-cy3 Fab) or dimeric anti-ICAM-1 (whole IgG of CBR-IC1/11 conjugated with cy3,

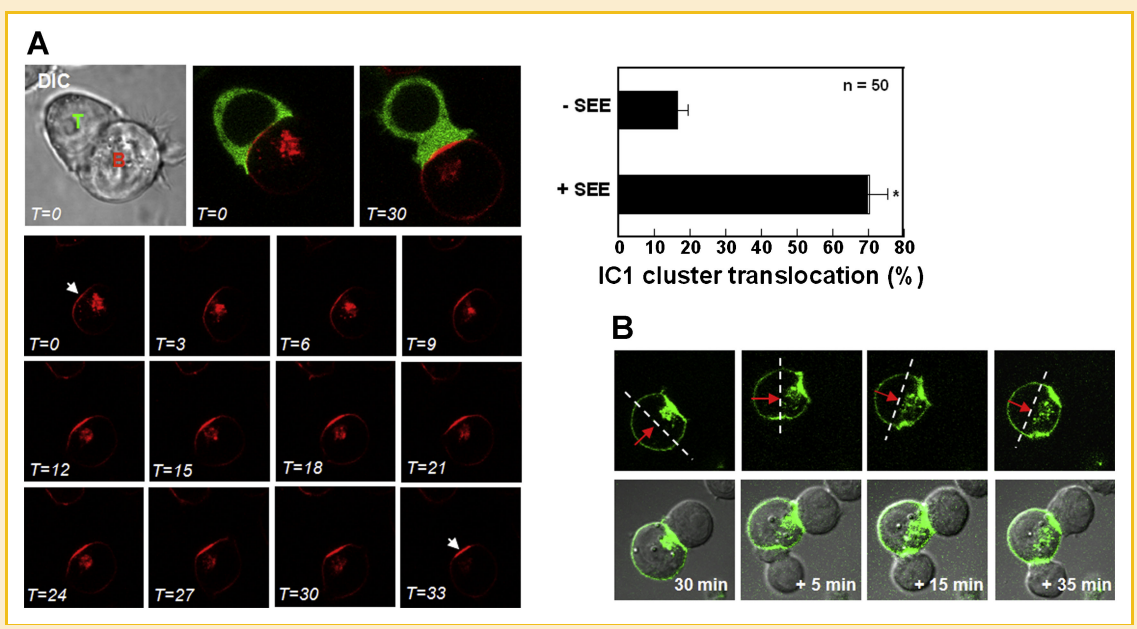

Fig. 1. Polarization and trafficking of internalized ICAM-1 to the T cell–APC contact zone. A: Raji B cells were stained with anti-IC1-cy3 Fab, pulsed with 5 μg/ml SEE, and incubated with Jurkat T cells expressing Swiprosin-1_GFP*. The distribution of ICAM-1 (red) was followed for 30 min by time-lapse confocal microscopy at 37°C. Images from a representative experiment were taken at 3-min intervals. See also Supplementary Video 1. *Note: Jurkat T cells were stably transfected with the Swiprosin-1_GFP gene for other experimental purposes. ICAM-1 (IC1) cluster translocation in APCs was quantified. A total of 50 conjugates were counted from three independent experiments. Data are means ± SD. *$P < 0.05$, as compared with non-SEE treated cells. B: Raji B cells were stained with anti-IC1-cy3 Fab and pulsed with SEE. After incubation with Jurkat T cells, the distribution of ICAM-1 was followed for 65 min by time-lapse confocal microscopy. Selected images are shown at 30, 35 (+5), 45 (+15), and 65 (+35) min of culture from a representative experiment. [Color figure can be viewed in the online issue, which is available at wileyonlinelibrary.com]

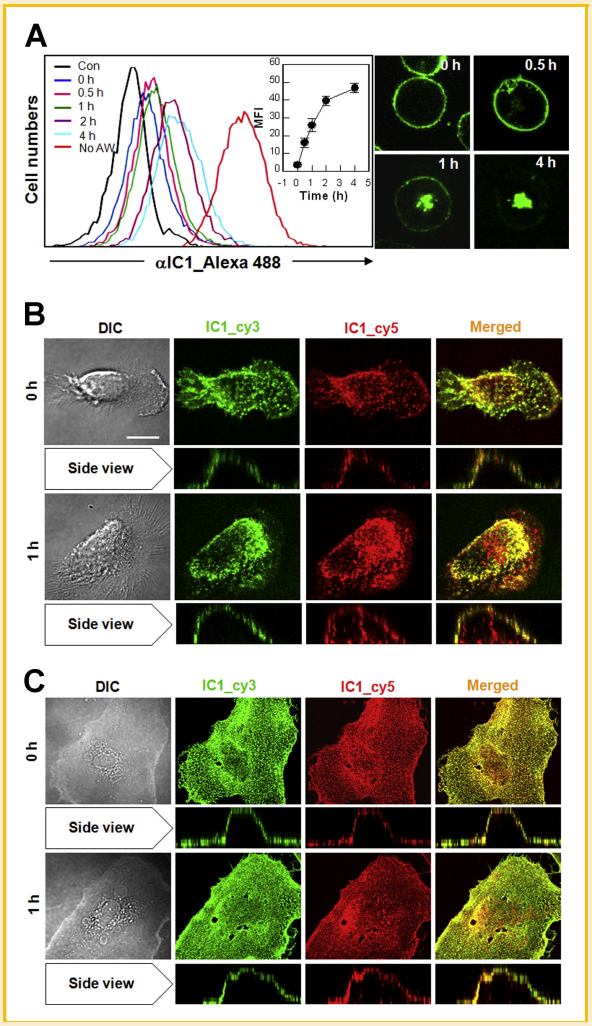

Fig. 2. Internalization of ICAM-1 in APCs, including Raji B cells and monocyte-derived DCs. A: Raji B cells were stained with anti-IC1-Alexa 488 IgG (for flow cytometry) or anti-IC1-cy3 Fab (for confocal microscopy) at 4°C for 1 h and cultured in a humidified 37°C incubator for internalization. Receptor internalization was quantified by flow cytometry and confocal microscopy. Note, Con = no antibody staining; AW = acid washing. B,C: Monocyte-derived matured human DCs (B) or HUVECs (C) were stained with anti-IC1-cy5 IgG at 37°C and subsequently stained with anti-IC1-cy3 Fab at 4°C. Scale bar = 10 μm. [Color figure can be viewed in the online issue, which is available at wileyonlinelibrary.com]

anti-IC1-cy3 IgG) antibody (data not shown). The only difference observed was that whole IgG was labeled to a higher degree than the Fab fragments, allowing for better detection of ICAM-1 in recycling endosomes, which were present at low levels (data not shown). Internalization could be seen as early as 30 min after incubation with anti-IC1-cy3 Fab, and reached a maximum level after 3–4 h (Fig. 2A). Because Raji B cells are a transformed cell line from a Burkitt's lymphoma patient, we extended the study to two primary cell types, human monocyte-derived DCs and human umbilical-vein endothelial cells (HUVECs). As shown in Figure 2B,C, anti-IC1-cy5 IgG was highly clustered in the cytosol of human DCs after 1 h of incubation, while only a few clusters were seen in the cytosol of HUVECs, as was previously reported [Muro et al., 2003, 2005]. These results suggest that internalization of ICAM-1 is not a result of antibody-mediated receptor clustering, but a naturally occurring event in APCs. In addition, APCs may have a better modulating mechanism for ICAM-1 internalization than do endothelial cells.

INTERNALIZATION OF ICAM-1 WAS MEDIATED BY THE NHE-DEPENDENT PATHWAY

Increased amounts of TCR in the recycling compartment before conjugate formation can facilitate TCR accumulation at the synapse [Das et al., 2004]. TCR internalization and accumulation in recycling endosomes are dependent on the PKC pathways [Minami et al., 1987; Alcover and Alarcon, 2000]. We also found that internalization of ICAM-1 was increased by PMA, but slightly reduced by PKC inhibitors, such as staurosporine and rottlein (Fig. 3A,a). Consistently, the efficiency of ICAM-1 accumulation at the immunological synapse was dependent on the amount of ICAM-1 in recycling endosomes before conjugate formation (Fig. 3A,b).

We further identified and manipulated cellular elements controlling the uptake and intracellular trafficking of ICAM-1 in APCs. Internalized ICAM-1 was not completely co-localized with the TfR, a delegate molecule in clathrin-mediated endocytosis, suggesting that APCs may not use this route for the internalization of ICAM-1 (Fig. 3B,a). Additionally, MDC, an inhibitor of clathrin-mediated endocytosis, did not inhibit the internalization of ICAM-1 (Fig. 3B,b). Interestingly, filipin, an inhibitor of caveolae-dependent endocytosis, was also not effective at inhibiting ICAM-1 internalization. Therefore, we considered other unique pathways for ICAM-1 internalization, rather than classical clathrin- or caveolae-dependent endocytosis.

Previous work has indicated that uptake of anti-ICAM-1 immunobeads in HUVECs was mediated by a member of the Na^+/H^+ exchanger (NHE) family [Muro et al., 2006]. Here, we asked whether APCs use the same mechanism to internalize surface ICAM-1 as HUVECs. ICAM-1 internalization is a spontaneously occurring event in APCs and therefore, may be different from that of HUVECs, in which internalization was triggered by antibody-conjugated immunobeads. AMR, an inhibitor of sodium/proton pumps, significantly inhibited internalization of ICAM-1 in Raji B cells (Fig. 3B,b). Since AMR is a potent inhibitor of additional ion channels, such as ENaC [Kleyman and Cragoe, 1988], we examined the effect of EIPA, another agent that alters sodium/proton exchange in cells, on ICAM-1 internalization. EIPA also significantly inhibited ICAM-1 internalization to a level comparable with that of AMR (Fig. 3B,b). Therefore, accumulation of ICAM-1 to the immunological synapse was significantly reduced by both inhibitors of NHE (Fig. 3B,c).

ICAM-1, PRESENT BOTH ON THE PLASMA MEMBRANE AND IN RECYCLING ENDOSOMES, WAS TARGETED TO THE T-CELL CONTACT ZONE

The data to this point demonstrate the importance of ICAM-1 internalization to ICAM-1 transport to the T-cell contact zone, but did not consider other potential mechanisms, including passive lateral diffusion [Favier et al., 2001] and cytoskeleton-mediated active movement [Wulfing et al., 1998] on the APC surface. To

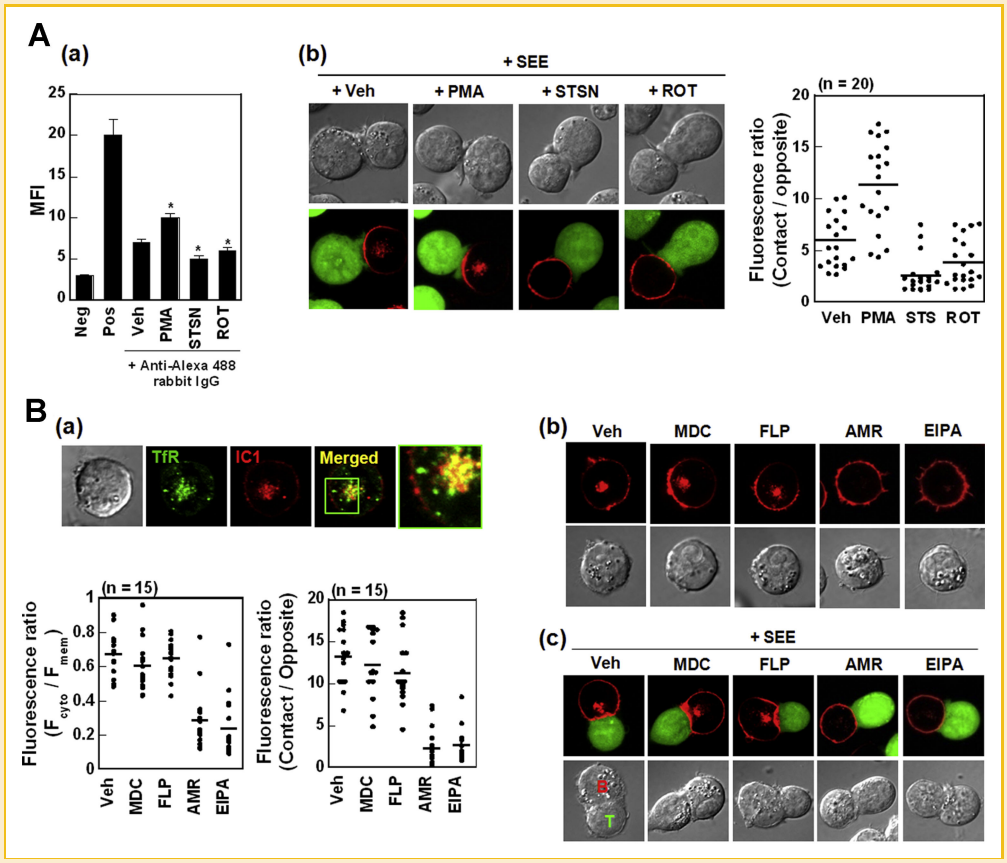

Fig. 3. Internalization of ICAM-1 was regulated by PKC and NHE-dependent pathways. A,a: Raji B cells were stained with anti-IC1-Alexa 488 IgG at 4°C, and then treated with 0.1% DMSO (Veh), 100 nM PMA, 500 nM staurosporine (STSN), or 10 μM rottlerin (ROT) at 37°C for 30 min. The remaining mIC1 was quenched by anti-Alexa 488-rabbit IgG. The MFI was measured by flow cytometry. Negative and positive controls consisted of non-stained or stained cells without quenching, respectively. $^{*}P < 0.05$, as compared with cells treated with vehicle alone. A,b: Raji B cells were stained with anti-IC1-cy3 IgG at 4°C, were treated with the reagents as described above at 37°C for 30 min, and then incubated with CMFDA-stained Jurkat T cells (green) for 30 min in the presence of 5 μg/ml SEE. The fluorescence ratio of contact/opposite was calculated. B,a: Raji B cells were stained with anti-IC1-cy3 IgG at 37°C. The cells were then fixed, permeabilized, stained with mouse anti-human transferrin receptor (TfR) antibody, and subsequently by a FITC-conjugated secondary antibody. Images were visualized by confocal microscopy. B,b: Raji B cells were pre-treated for 30 min with 50 μM MDC, 1 μg/ml filipin (FLP), 100 μM AMR, or 20 μM EIPA. The cells were stained with anti-IC1-cy3 IgG at 4°C and then cultured at 37°C for 2 h for internalization. B,c: Raji B cells from (b) were loaded with 5 μg/ml SEE and incubated with CMFDA-stained Jurkat T cells (green) for 30 min. The fluorescence intensity due to the internalization or accumulation at the T cell–APC contact site was quantified. Each dot represents a single cell (b) and a T cell–APC conjugate (c). At least 15 cells were examined from each treatment group. AMR, $P < 0.05$; EIPA, $P < 0.05$, as compared with cells treated with vehicle alone. [Color figure can be viewed in the online issue, which is available at wileyonlinelibrary.com]

this end, cIC1 and mIC1 were labeled with anti-IC1-cy5 IgG and anti-IC1-cy3 Fab, respectively, and visualized by confocal microscopy. In the presence of superantigen, both mIC1 and cIC1 accumulated at significant levels at the T-cell contact zone (Fig. 4A). The two signals largely overlapped at the contact zone, thereby suggesting that surface ICAM-1 corresponded to ICAM-1 accumulation in the immunological synapse.

We next examined the factors that could regulate surface ICAM-1 movement to the T-cell contact zone. The potential involvement of the actin cytoskeleton was tested since actin plays a critical role in T-cell morphology and movement, including formation of the immunological synapse resulting in T-cell activation [Dustin and Cooper, 2000; Huang and Burkhardt, 2007]. mIC1 was stained with only anti-IC1-cy3 Ig at 4°C. As shown in Figure 4B, movement of mIC1 was significantly retarded by treatment with the actin disrupting agents CB and latrunculin A, suggesting that cytoskeleton-mediated active movement, but not passive lateral diffusion, could explain surface ICAM-1 transport to the immunological synapse.

Since earlier reports demonstrated that native ICAM-1 protein is associated with the actin-containing microfilament network and that their interaction is mediated by the cytoplasmic domain of ICAM-1 [Carpen et al., 1992; Carman et al., 2003], we further examined whether ICAM-1 movement required an intact cytoplasmic domain. Interestingly, as compared to wild-type ICAM-1, deletion of the cytoplasmic domain significantly reduced ICAM-1 accumulation at the T-cell contact zone (Fig. 4C). This finding led us to examine whether the reduced accumulation of IC1ΔCTD_GFP was due to the reduced lateral mobility of mIC1. We compared the dynamics of two ICAM-1 constructs by FRAP of an area within and without the T-cell contact zone. We found that the average FRAP velocity of wt-IC1_GFP was much slower than that of IC1ΔCTD_GFP ($t_{1/2} = 49.53 \pm 2.84$ vs. 29.50 ± 1.08). In addition, the mobile fraction of wt-IC1_GFP was smaller than that of IC1ΔCTD_GFP

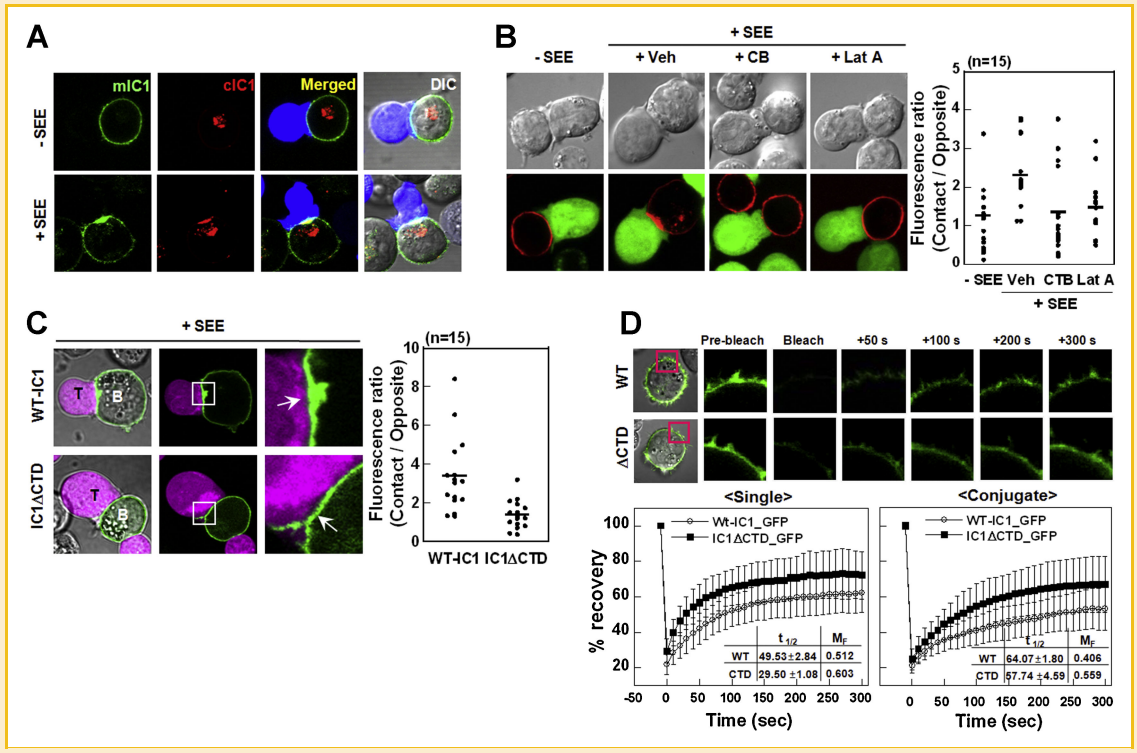

Fig. 4. ICAM-1 present on the plasma membrane or in recycling endosomes was targeted to the T-cell contact zone. A: Both cytosolic (cIC1) and membrane (mIC1) ICAM-1 in Raji B cells was labeled with anti-IC1-cy5 IgG and anti-IC1-cy3 Fab, respectively. The cells were then pulsed with or without 5 μg/ml SEE and incubated with CMFDA-stained Jurkat T cells (blue) for 30 min. B: Raji B cells were pre-treated with 1 μg/ml cytochalasin B (CB) and 1 μg/ml latrunculin A (Lat A) at 37°C for 30 min. Membrane ICAM-1 was then stained with anti-IC1-cy3 IgG at 4°C. After conjugation with SEE-pulsed Jurkat T cells for 30 min, the fluorescent intensity ratio of contact/opposite was quantified. C: Raji B cells expressing wt-IC1_GFP or IC1ΔCTD_GFP were incubated with Jurkat T cells (CMRA) in the absence or presence of SEE. A magnification of the boxed regions is shown in the right panels. Arrows indicate the distinctive accumulation of ICAM-1 at the contact site of the T cell–APC. For B and C, each dot represents a T cell–APC conjugate. At least 15 cells were examined from each reagent treatment. CB, $P < 0.05$; Lat A, $P < 0.05$, as compared with cells treated with vehicle alone. D: Both ligand-free (single) and ligand-engaged (conjugate) wt-IC1_GFP are less mobile than the IC1ΔCTD_GFP. Raji B cells were incubated with or without SEE-pulsed Jurkat T cells for 30 min. A selected area (2 μm square) of the IC1_GFP on the membrane was photobleached, and fluorescence recovery was monitored. Images at representative time points are shown. Bleaching recovery kinetics are represented as the percentage of FRAP. Data are representative of three individual experiments. [Color figure can be viewed in the online issue, which is available at wileyonlinelibrary.com]

($M_F = 0.512$ vs. 0.603; Fig. 4D). These results demonstrated that rapid lateral passive diffusion does not enhance ICAM-1 accumulation at the immunological synapse. FRAP was also performed within the T cell–APC contact zone after synapse formation. Interestingly, the average FRAP velocities of both ICAM-1 constructs were slowed at the T-cell contact zone ($t_{1/2} = 64.07 \pm 1.80$ s vs. 57.74 ± 4.59 s; Fig. 4D), suggesting that the two forms of ICAM-1 were under LFA-1 constraint. Taken together, these results suggest that passive lateral diffusion was not the mechanism of immunological synapse formation. Instead, cytoskeleton-dependent active transport could be a mechanism for mIC1 transport to the T-cell contact zone.

AFFINITY CHANGE OF LFA-1 ON T CELLS WAS ESSENTIAL FOR BOTH ICAM-1 AND MHC CLASS II TRAFFICKING TO THE T-CELL CONTACT ZONE

We next examined whether targeting of ICAM-1 to the immunological synapse through the polarized recycling compartment was dependent on antigen-stimulated TCR engagement of MHC, or if it required only LFA-1 affinity changes on T cells. As shown in Figure 5, both mIC1 and cIC1 accumulated at the contact zone in response to the activating antibody CBR-LFA-1/2 [Oh et al., 2007] even in the absence of superantigen. However, this accumulation was dramatically blocked by the blocking antibody TS1/22 [Sanchez-Madrid et al., 1982]. These results suggest that polarization and ICAM-1 transportation to the immunological synapse was not dependent on antigen, but was mediated by high-affinity LFA-1 on T cells.

MHC class II molecules accumulate in intraluminal vesicles of multivesicular antigen-processing compartments before trafficking to the plasma membrane [Adam et al., 2009]. Therefore, we examined whether internalized ICAM-1 was co-localized with MHC class II molecules in the recycling compartment, as well as at the immunological synapse of the antigen-recognizing T-cell contact. As shown in Figure 6A, ICAM-1, both within the APC and at the T-cell contact zone, was largely co-localized with MHC class II molecules. The corresponding co-localization percentages in the absence or presence of SEE are 71.1% and 82.1%, respectively. Moreover, approximately 70% of T cell–APC conjugates formed in the presence of SEE indicated polarization of each molecule in the contact zone (Fig. 6A).

Based on this observation, we further examined whether trafficking and accumulation of MHC class II at the immunological

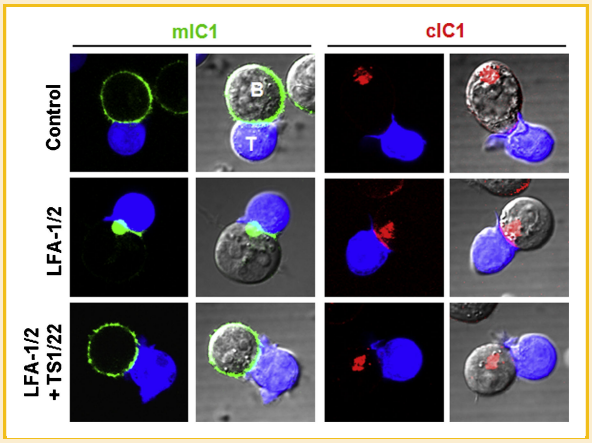

Fig. 5. A change in LFA-1 affinity on T cells was essential for ICAM-1 trafficking to the T-cell contact zone. Raji B cells were labeled with anti-IC1-cy5 IgG for cIC1 and anti-IC1-cy3 Fab for mIC1. The cells were treated with 10 μg/ml LFA-1/2 (activation antibody) or 10 μg/ml LFA-1/2 plus TS1/22 (blocking antibody), and incubated for 30 min at 37°C with CMFDA-stained Jurkat T cells (blue). The distribution of mIC1 or cIC1 was visualized by confocal microscopy. [Color figure can be viewed in the online issue, which is available at wileyonlinelibrary.com]

synapse could also be mediated by high-affinity LFA-1. To this end, we examined the accumulation of MHC class II molecules in the APC after incubation with three different T-cell types, Jurkat T cells, PBLT cells, and S-PBLT cells. Surprisingly, adhesion of all three T cells to the Raji B cells by the LFA-1/2 antibody dramatically induced not only asymmetrical polarization of the recycling compartment, but also accumulation of MHC class II at the immunological synapse (Fig. 6B). Moreover, treatment with the blocking antibody TS1/22 significantly blocked superantigen-induced accumulation of MHC class II at the immunological synapse (Fig. 6C). These results strongly suggest that the affinity status of LFA-1 determines the efficacy of SMAC molecule trafficking to the immunological synapse during antigen-stimulated T-cell contact.

One interesting point to note is that among the three different T-cell types examined, PBLT cells induced the smallest amount of translocation of MHC class II clusters to the T-cell contact. Since the expression of adhesion molecules varies dramatically between different cell states and types, we further examined whether induction of asymmetric polarization of MHC class II (or ICAM-1) to the T-cell contact zone was correlated with the expression levels of LFA-1 and/or ICAM-1 molecules on T cells or if size also partially contributed, as PBLT cells are much smaller than other two T-cell types. As shown in Figure 6D, PBLT cells expressed relatively higher levels of receptors than did Jurkat T cells or S-PBLT cells. These results suggest that spatial occupation by cell size is also an important factor for the asymmetric polarization of internal MHC class II (or ICAM-1) clusters to the immunological synapse.

ICAM-1 TARGETING TO THE IMMUNOLOGICAL SYNAPSE WAS MEDIATED BY THE MICROTUBULE AND ACTIN CYTOSKELETON AND WAS LINKED TO ENDOLYSOSOME-RELATED VESICLE TRAFFICKING

In T cells encountering stimulatory APCs, the MTOC translocates to the area adjacent to the APC. Microtubules, which extend from the MTOC to the APC contact zone, help to deliver TCR-containing endocytic vesicles to the immunological synapse [Das et al., 2004]. Therefore, we examined whether internalized ICAM-1 also co-localized with MTOC in APCs. mIC1 was poorly co-localized with the tubulin tracker in Raji B cells (Fig. 7A). However, after incubation for 3 h at 37°C, internalized ICAM-1 showed increased co-localization with the tubulin tracker. In addition, both the tubulin tracker and ICAM-1 was heavily polarized to the T-cell contact zone in the presence of superantigen (Fig. 7B). This suggests that the MTOC functions to deliver ICAM-1-containing endocytic vesicles to the immunological synapse in APCs. After 60 min of T-cell contact, most of the ICAM-1 had accumulated at the immunological synapse, while ICAM-1 in the MTOC was proportionally decreased (Fig. 7B). Consistently, cells treated with COL displayed impaired polarization of recycling endosomes toward the T-cell contact site and reduced accumulation of ICAM-1 at the immunological synapse (Fig. 7C). We also examined whether actin disruption inhibited the polarization of recycling compartments toward the T-cell contact zone. Pre-treatment with CB or Lat A dramatically inhibited not only polarization of the recycling compartment, but also accumulation of ICAM-1 at the immunological synapse (Fig. 7C). Wortmannin, a PI3-kinase inhibitor, revealed no inhibitory effect (Fig. 7C), suggesting that the PI3-kinase pathway was not involved in ICAM-1 trafficking to the immunological synapse.

To extend our study to non-transformed APCs, a similar experiment was carried out using human monocyte-derived DCs with anti-IC1-cy3 Fab-labeled ICAM-1. LFA-1 on S-PBLT cells was labeled with the anti-LFA-1-Alexa 488 IgG. In contrast to the Jurkat T–Raji B cell conjugates, the large ICAM-1 cluster was not dramatically reoriented to the S-PBLT cell contact zone even in the presence of SEB. Nevertheless, small intracellular clusters containing anti-ICAM-1 mAb were significantly polarized and apposed to the T-cell contact site in the presence of SEB (Fig. 8A). The function of the microtubule and actin cytoskeletons was also examined in primary DCs. Unexpectedly, most of the cIC1 (internalized form) in DCs was in extended tubular structures and was extremely mobile (0.72 ± 0.23 μm/s) with bidirectional movement (Fig. 8B and Supplementary Video 2A). These specialized structures were likely tubular endosomes of matured DCs as previously reported [Boes et al., 2002; Chow et al., 2002]. MHC class II molecules are highly enriched in these tubular structures which appear to be responsible for the transport of MHC class II molecules from the endosomal compartment to the cell surface [Boes et al., 2002; Chow et al., 2002]. Treatment with COL or CB significantly disrupted the tubular structures and reduced the mobility of cIC1 (0.03 ± 0.01 and 0.03 ± 0.02 μm/s, respectively; Fig. 8B and Supplementary Videos 2B and C). In contrast to cIC1, surface ICAM-1 was immobile and stable while engaged with LFA-1 on T cells (Fig. 8C).

DISCUSSION

Accumulation and segregation of TCR complexes, including TCRs, co-receptors, adhesion molecules, and signaling and cytoskeletal components, into supramolecular clusters are essential steps for dynamic spatial and temporal communication with APCs and

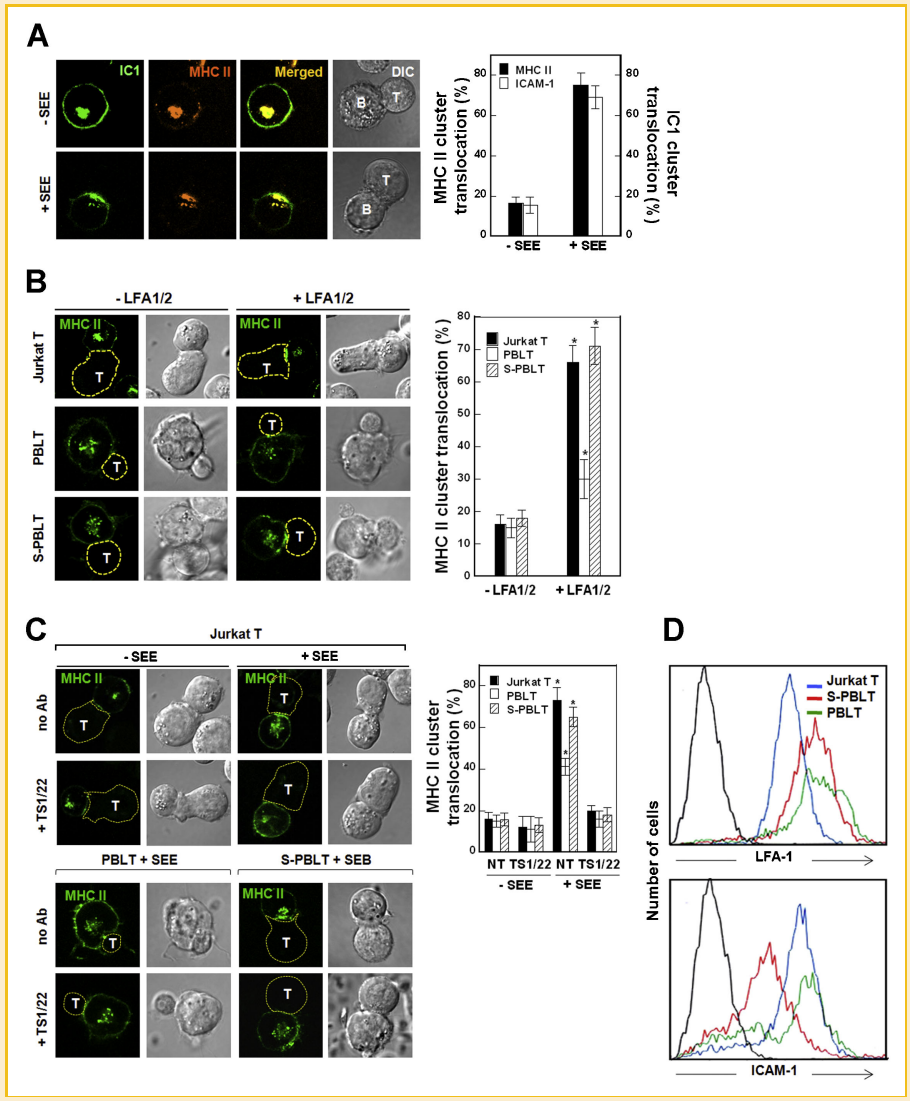

Fig. 6. A change in LFA-1 affinity on T cells was essential for MHC class II trafficking to the T-cell contact zone. A: ICAM-1 was co-localized with MHC class II inside APCs. Raji cells were stained with anti-HLA-DR-PE-cy5.5 IgG and anti-IC1-cy3 Fab. The cells were then pulsed with or without 5 μg/ml SEE and incubated with Jurkat T cells for 30 min. Translocation of ICAM-1 and MHC class II clusters was quantified. B,C: Raji B cells were labeled with anti-HLA-DR-PE-cy5.5 mAb. The cells were then pulsed with or without 10 μg/ml LFA-1/2 (C), 5 μg/ml SEE, or 0.5 μg/ml SEB (D), and incubated for 30 min with Jurkat T, PBLT, or S-PBLT cells in the presence or absence of 10 μg/ml TS1/22. Images were visualized by confocal microscopy. MHC class II translocation was quantified. A total of 50 conjugates were counted from three independent experiments. Data are means ± SD. $^{*}P < 0.05$, as compared with cells without SEE treatment. D: The objective cells (Jurkat T, PBLT, and S-PBLT) were stained with anti-IC1-cy3 IgG (CBR1C1/11) or anti-LFA-1-cy3 IgG (TS1/22) and the fluorescence intensities were measured by flow cytometry. [Color figure can be viewed in the online issue, which is available at wileyonlinelibrary.com]

efficient T-cell activation. Thus, the pathways and mechanisms by which T-cell molecules accumulate at the immunological synapse have been the subjects of extensive investigation [Das et al., 2004; Cairo et al., 2006; Kaizuka et al., 2007; Nolz et al., 2007]. In contrast, trafficking of SMAC molecules, excluding MHC classes I and II molecules, to the APC immunological synapse has been unclear because it may be partially controlled by the interacting T cell. However, the present results unambiguously demonstrate that APCs also play an active role in transporting SMAC molecules to the immunological synapse. To be targeted to the T cell–APC contact zone, microtubule and actin-dependent asymmetrical transport of SMAC molecules in APCs was required because the recycling compartment was only polarized toward the T-cell contact site in the presence of antigen peptide. The LFA-1–ICAM-1 interaction played a pivotal role for the asymmetrical transport of both ICAM-1 and MHC class II through the cell interior of APCs.

Activated T cells can recruit exosomes secreted by DCs via LFA-1 [Nolte-'t Hoen et al., 2009]. Since DC exosomes are secreted vesicles formed within multivesicular bodies [Davis, 2007], both exosomes and polarized recycling compartments may share the same route to reach to the T-cell contact. Thus, complete blocking of exosome binding to the activated T cells with anti-LFA-1 [Nolte-'t Hoen et al., 2009] strongly implies that the LFA-1–ICAM-1 interaction is also critical for transport of SMAC molecules, including MHC class II and ICAM-1, to the immunological synapse in APCs. Therefore, it will be interesting to examine whether transportation of other SMAC

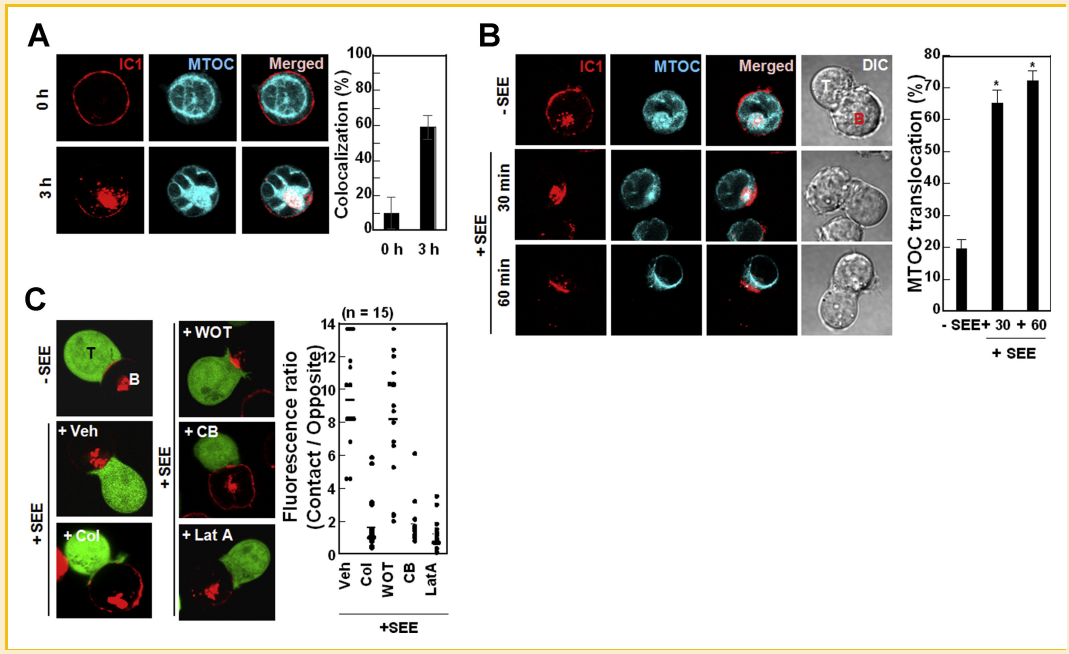

Fig. 7. Trafficking of ICAM-1 was mediated by microtubule and actin cytoskeletons. A,B: Raji B cells were stained with tubulin tracker (cyan) and anti-IC1-cy3 Fab (red). The cells were then cultured at 37°C for 3 h (A), pulsed with 5 μg/ml SEE, and incubated with Jurkat T cells for 30 or 60 min (B). Colocalization (%) values were calculated by FLUOVIEW software. MTOC translocation was quantified from 50 conjugates from three independent experiments. Data are means ± SD. *$P < 0.05$, as compared with cells without SEE treatment. C: Raji B cells were stained with anti-IC1-cy3 IgG. The cells were treated with 1 μg/ml colchicine (COL), 0.5 μM wortmannin (WOT), 1 μg/ml cytochalasin B (CB), and 1 μg/ml latrunculin A (Lat A) for 30 min and were further cultured with CMFDA-stained Jurkat T cells for 30 min with or without 5 μg/ml SEE. The fluorescent intensity ratio of contact/opposite was quantified. Col, $P < 0.05$; CB, $P < 0.05$; Lat A, $P < 0.05$, as compared with cells treated with vehicle (0.1% DMSO) alone. [Color figure can be viewed in the online issue, which is available at wileyonlinelibrary.com]

molecules to the immunological synapse is also mediated by the LFA-1–ICAM-1 interaction. Antibody-stained cytosolic MHC class II clusters were not oriented toward the T cell–APC contact site if T cells were pre-incubated with anti-LFA-1 blocking antibody. This strongly suggests that the LFA-1–ICAM-1 interaction plays an important role in the polarization of the recycling compartment and the subsequent trafficking of SMAC molecules to the immunological synapse in APCs.

In mature DCs the clustering of MHC class II molecules is induced by ICAM-3, and to a lesser extent by ICAM-1, both of which were expressed on T cells or on ICAM-1-coated latex beads [de la Fuente et al., 2005]. Interestingly, the molecular set for MHC class II clustering in mature DCs is in a reversed configuration of that seen in the present study. Similar to what was seen in this study, MHC class II clustering was significantly reduced by a LFA-1 blockade with the anti-LFA-1 mAb [de la Fuente et al., 2005]. However, the previous work by de la Fuente et al. was different from the present study in the following two aspects. First, it was suggested that ICAM-3 binding to LFA-1 on DCs was only required for the initial scanning of the APC surface by T cells in the absence of antigen. Second, only the existence of an adhesion-dependent component in MHC class II lateral mobility on DC membranes was determined, but whether this interaction could induce asymmetrical polarization of internal MHC class II clusters in DCs was not considered.

Induction of asymmetrical polarization of SMAC molecules and MTOC translocation may require stronger interactions between T cells and APCs. Interestingly, we found that PBLT cells, which express higher levels of LFA-1 and ICAM-1 than Jurkat T or S-PBLT cells, induced the lowest levels of MHC class II cluster translocation. These results strongly suggest that the size of adhered T cells and their spatial occupation on APCs are also critical for the asymmetrical induction of SMAC molecules, including MHC class II and ICAM-1. One interesting point to note is that LFA-1 in DCs may also follow the same route of transport to the T-cell contact site as was taken by ICAM-1 or MHC class II. Further studies will be necessary to elucidate the molecular mechanism of how activating T-cell LFA-1 has such a profound effect on the trafficking of ICAM-1 and MHC class II in the APC.

Surface ICAM-1 was efficiently internalized into the cytosol in both Raji B cells and human monocyte-derived DCs. This finding was striking because a previous report demonstrated that monomeric (Fab) anti-ICAM-1 and anti-PECAM-1 were not internalized by endothelial cells [Muro et al., 2003]. Endothelial cells internalize natural ligands and artificial macromolecular ligands designed to be carriers for specific drugs and gene delivery [Jacobson et al., 1996; Spragg et al., 1997; Danilov et al., 2001]. In addition, it is becoming apparent that ICAM-1 serves as a plasma membrane receptor to mediate internalization of natural ligands by endothelial cells [Diamond et al., 1990; Kumasaka et al., 1996]. Importantly, however, the requirement of multivalent anti-ICAM-1 conjugates or nanocarriers by endothelial cells versus the naturally occurring event in APCs, suggests that the two cell types evolved differently in terms of receptor internalization. Nonetheless, the fact that both cell types utilized the same mechanism to internalize both monomeric

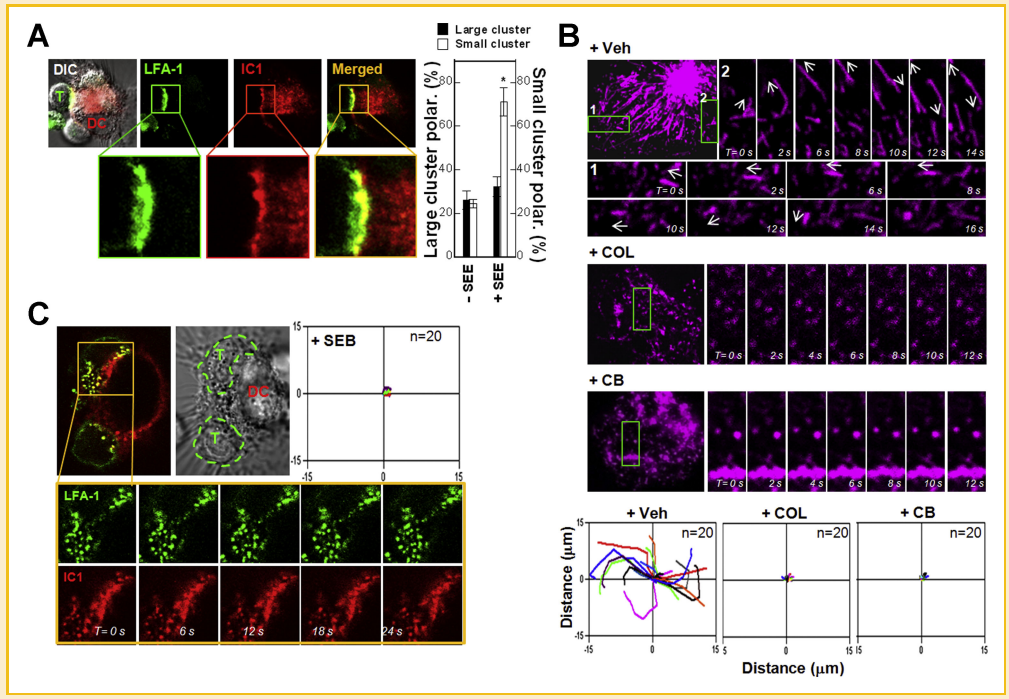

Fig. 8. Polarization and trafficking of ICAM-1 in human DCs. A: S-PBLT cells and human DCs were stained with anti-LFA-1 (TS2/4)-Alexa 488 IgG or anti-IC1-cy3 IgG, respectively. S-PBLT cells were then incubated with DCs in the presence or absence of 0.5 μg/ml SEB. After a 30-min incubation, images were taken by confocal microscopy and large and small ICAM-1 cluster translocations were quantified. A total of 50 conjugates were counted from three independent experiments. Data are means ± SD. $^{*}P < 0.05$, as compared with cells without SEE treatment. B: Human DCs were stained with anti-IC1-cy3 IgG. The cells were treated with 0.1% DMSO (Veh), 1 μg/ml colchicine (COL), or 1 μg/ml CB for an additional 30 min. C: Human DCs were stained with anti-IC1-cy3 IgG and incubated for 30 min with S-PBLT cells (stained with anti-LFA-1-Alexa 488 IgG) in the presence of 0.5 μg/ml SEB. The movement of ICAM-1 was followed for 1 min by time-lapse confocal microscopy at 37°C. Selected images are shown at every 2–6 s of culture from a representative experiment. See also Supplementary Videos 2A–C for (B). Migratory distance of each ICAM-1 cluster (each line) was calculated by Metamorpho offline version 7.6.0.0. One representative experiment out of at least three independent experiments is shown. [Color figure can be viewed in the online issue, which is available at wileyonlinelibrary.com]

and multimeric forms of ICAM-1 [Muro et al., 2003, 2005, 2006] is interesting. Further study will be required to fully understand the mechanism of ICAM-1 internalization, which may be different for APCs and endothelial cells.

The results presented in this work also demonstrate the existence of another mechanism of ICAM-1 transport to the T-cell contact zone: cytoskeleton-driven movement on the cell surface. Passive lateral diffusion does not likely correspond to ICAM-1 transport as deletion of the cytoplasmic domain revealed reduced accumulation at the T-cell contact zone and more rapid lateral movement than the wild-type. In addition, ICAM-1 accumulation at the T-cell contact area was significantly impaired when actin was disrupted, even though, in this case, membrane-bound ICAM-1 was more laterally mobile than the native form (data not shown). As consistent with our present study, previous reports demonstrated an active, cytoskeletal mechanism that drives receptor accumulation at the T cell–APC interface [Wulfing and Davis, 1998]. However, whether surface and intracellular transport of ICAM-1 occurs simultaneously or sequentially during the formation of the immunological synapse and whether these mechanisms are differentially regulated will need further investigation.

Highly mobile ICAM-1 was in a tubular form in DCs (0.87 ± 0.13 μm/s; Fig. 8B), suggesting that internalized ICAM-1 was integrated into the dynamic endolysosomal tubules for translocation to the cell surface to engage LFA-1 on T cells. Consistent with our findings, previous reports also demonstrated that DCs generate tubules from lysosomal compartments that fuse directly with the plasma membrane [Boes et al., 2002; Chow et al., 2002]. Moreover, intracellular movement of this tubular structure was dynamic (up to 2 μm/s), as changes in location could be observed in confocal images captured only seconds apart [Boes et al., 2002]. Thus, it is not surprising that this tubular structure collapses in response to treatment with a microtubule disrupting agent as a previous report also demonstrated that transport of MHC II-EGFP-positive tubules were strictly microtubule-dependent [Boes et al., 2002]. Overall, current data strongly suggests that the translocation of endosomal ICAM-1 to the cell surface is mediated by the same mechanism by which peptide-loaded MHC class II molecules engage Ag-specific T cells.

In summary, ICAM-1 can be transported to the immunological synapse via two major pathways: (1) through the cell interior by recycling endosomes and (2) on the cell surface by cytoskeleton-dependent active transport. The former requires continuous endocytosis and recycling of ICAM-1 and LFA-1-dependent polarization of the recycling endolysosomal compartment. In both cases, induction of a high-affinity state of LFA-1 on T cells is critical to initiate targeted movement of ICAM-1 to the immunological synapse. Interestingly, the affinity status of LFA-1 also determines

MHC class II trafficking to the immunological synapse during antigen-stimulated T-cell contact.

REFERENCES

Adam RD, Elliott SP, Taljanovic MS. 2009. The spectrum and presentation of disseminated coccidioidomycosis. Am J Med 122:770–777.

Alcover A, Alarcon B. 2000. Internalization and intracellular fate of TCR-CD3 complexes. Crit Rev Immunol 20:325–346.

Blanchard N, Di Bartolo V, Hivroz C. 2002. In the immune synapse, ZAP-70 controls T cell polarization and recruitment of signaling proteins but not formation of the synaptic pattern. Immunity 17:389–399.

Boes M, Cerny J, Massol R, Op den Brouw M, Kirchhausen T, Chen J, Ploegh HL. 2002. T-cell engagement of dendritic cells rapidly rearranges MHC class II transport. Nature 418:983–988.

Cairo CW, Mirchev R, Golan DE. 2006. Cytoskeletal regulation couples LFA-1 conformational changes to receptor lateral mobility and clustering. Immunity 25:297–308.

Campi G, Varma R, Dustin ML. 2005. Actin and agonist MHC-peptide complex-dependent T cell receptor microclusters as scaffolds for signaling. J Exp Med 202:1031–1036.

Carman CV, Jun CD, Salas A, Springer TA. 2003. Endothelial cells proactively form microvilli-like membrane projections upon intercellular adhesion molecule 1 engagement of leukocyte LFA-1. J Immunol 171:6135–6144.

Carpen O, Pallai P, Staunton DE, Springer TA. 1992. Association of intercellular adhesion molecule-1 (ICAM-1) with actin-containing cytoskeleton and alpha-actinin. J Cell Biol 118:1223–1234.

Chow A, Toomre D, Garrett W, Mellman I. 2002. Dendritic cell maturation triggers retrograde MHC class II transport from lysosomes to the plasma membrane. Nature 418:988–994.

Danilov SM, Gavrilyuk VD, Franke FE, Pauls K, Harshaw DW, McDonald TD, Miletich DJ, Muzykantov VR. 2001. Lung uptake of antibodies to endothelial antigens: Key determinants of vascular immunotargeting. Am J Physiol Lung Cell Mol Physiol 280:L1335–L1347.

Das V, Nal B, Dujeancourt A, Thoulouze MI, Galli T, Roux P, Dautry-Varsat A, Alcover A. 2004. Activation-induced polarized recycling targets T cell antigen receptors to the immunological synapse; Involvement of SNARE complexes. Immunity 20:577–588.

Davis DM. 2007. Intercellular transfer of cell-surface proteins is common and can affect many stages of an immune response. Nat Rev Immunol 7:238–243.

de la Fuente H, Mittelbrunn M, Sanchez-Martin L, Vicente-Manzanares M, Lamana A, Pardi R, Cabanas C, Sanchez-Madrid F. 2005. Synaptic clusters of MHC class II molecules induced on DCs by adhesion molecule-mediated initial T-cell scanning. Mol Biol Cell 16:3314–3322.

Diamond MS, Staunton DE, de Fougerolles AR, Stacker SA, Garcia-Aguilar J, Hibbs ML, Springer TA. 1990. ICAM-1 (CD54): A counter-receptor for Mac-1 (CD11b/CD18). J Cell Biol 111:3129–3139.

Dustin ML, Cooper JA. 2000. The immunological synapse and the actin cytoskeleton: Molecular hardware for T cell signaling. Nat Immunol 1:23–29.

Egen JG, Allison JP. 2002. Cytotoxic T lymphocyte antigen-4 accumulation in the immunological synapse is regulated by TCR signal strength. Immunity 16:23–35.

Favier B, Burroughs NJ, Wedderburn L, Valitutti S. 2001. TCR dynamics on the surface of living T cells. Int Immunol 13:1525–1532.

Gorska MM, Liang Q, Karim Z, Alam R. 2009. Uncoordinated 119 protein controls trafficking of Lck via the Rab11 endosome and is critical for immunological synapse formation. J Immunol 183:1675–1684.

Grakoui A, Bromley SK, Sumen C, Davis MM, Shaw AS, Allen PM, Dustin ML. 1999. The immunological synapse: A molecular machine controlling T cell activation. Science 285:221–227.

Huang Y, Burkhardt JK. 2007. T-cell-receptor-dependent actin regulatory mechanisms. J Cell Sci 120:723–730.

Jacobson BS, Stolz DB, Schnitzer JE. 1996. Identification of endothelial cell-surface proteins as targets for diagnosis and treatment of disease. Nat Med 2:482–484.

Kaizuka Y, Douglass AD, Varma R, Dustin ML, Vale RD. 2007. Mechanisms for segregating T cell receptor and adhesion molecules during immunological synapse formation in Jurkat T cells. Proc Natl Acad Sci USA 104:20296–20301.

Kleyman TR, Cragoe EJ, Jr. 1988. Amiloride and its analogs as tools in the study of ion transport. J Membr Biol 105:1–21.

Kuhne MR, Lin J, Yablonski D, Mollenauer MN, Ehrlich LI, Huppa J, Davis MM, Weiss A. 2003. Linker for activation of T cells, zeta-associated protein-70, and Src homology 2 domain-containing leukocyte protein-76 are required for TCR-induced microtubule-organizing center polarization. J Immunol 171:860–866.

Kumasaka T, Quinlan WM, Doyle NA, Condon TP, Sligh J, Takei F, Beaudet A, Bennett CF, Doerschuk CM. 1996. Role of the intercellular adhesion molecule-1 (ICAM-1) in endotoxin-induced pneumonia evaluated using ICAM-1 antisense oligonucleotides, anti-ICAM-1 monoclonal antibodies, and ICAM-1 mutant mice. J Clin Invest 97:2362–2369.

Kupfer A, Swain SL, Janeway CA, Jr., Singer SJ. 1986. The specific direct interaction of helper T cells and antigen-presenting B cells. Proc Natl Acad Sci USA 83:6080–6083.

Minami Y, Samelson LE, Klausner RD. 1987. Internalization and cycling of the T cell antigen receptor. Role of protein kinase C. J Biol Chem 262:13342–13347.

Monks CR, Freiberg BA, Kupfer H, Sciaky N, Kupfer A. 1998. Three-dimensional segregation of supramolecular activation clusters in T cells. Nature 395:82–86.

Munoz P, Mittelbrunn M, de la Fuente H, Perez-Martinez M, Garcia-Perez A, Ariza-Veguillas A, Malavasi F, Zubiaur M, Sanchez-Madrid F, Sancho J. 2008. Antigen-induced clustering of surface CD38 and recruitment of intracellular CD38 to the immunologic synapse. Blood 111:3653–3664.

Muro S, Wiewrodt R, Thomas A, Koniaris L, Albelda SM, Muzykantov VR, Koval M. 2003. A novel endocytic pathway induced by clustering endothelial ICAM-1 or PECAM-1. J Cell Sci 116:1599–1609.

Muro S, Gajewski C, Koval M, Muzykantov VR. 2005. ICAM-1 recycling in endothelial cells: A novel pathway for sustained intracellular delivery and prolonged effects of drugs. Blood 105:650–658.

Muro S, Mateescu M, Gajewski C, Robinson M, Muzykantov VR, Koval M. 2006. Control of intracellular trafficking of ICAM-1-targeted nanocarriers by endothelial Na+/H+ exchanger proteins. Am J Physiol Lung Cell Mol Physiol 290:L809–L817.

Nolte-'t Hoen EN, Buschow SI, Anderton SM, Stoorvogel W, Wauben MH. 2009. Activated T cells recruit exosomes secreted by dendritic cells via LFA-1. Blood 113:1977–1981.

Nolz JC, Medeiros RB, Mitchell JS, Zhu P, Freedman BD, Shimizu Y, Billadeau DD. 2007. WAVE2 regulates high-affinity integrin binding by recruiting vinculin and talin to the immunological synapse. Mol Cell Biol 27:5986–6000.

Oh HM, Lee S, Na BR, Wee H, Kim SH, Choi SC, Lee KM, Jun CD. 2007. RKIKK motif in the intracellular domain is critical for spatial and dynamic organization of ICAM-1: Functional implication for the leukocyte adhesion and transmigration. Mol Biol Cell 18:2322–2335.

Patino-Lopez G, Dong X, Ben-Aissa K, Bernot KM, Itoh T, Fukuda M, Kruhlak MJ, Samelson LE, Shaw S. 2008. Rab35 and its GAP EPI64C in T cells regulate receptor recycling and immunological synapse formation. J Biol Chem 283:18323–18330.

Sanchez-Madrid F, Krensky AM, Ware CF, Robbins E, Strominger JL, Burakoff SJ, Springer TA. 1982. Three distinct antigens associated with human T-lymphocyte-mediated cytolysis: LFA-1, LFA-2, and LFA-3. Proc Natl Acad Sci USA 79:7489–7493.

Spragg DD, Alford DR, Greferath R, Larsen CE, Lee KD, Gurtner GC, Cybulsky MI, Tosi PF, Nicolau C, Gimbrone MA, Jr. 1997. Immunotargeting of liposomes to activated vascular endothelial cells: A strategy for site-selective delivery in the cardiovascular system. Proc Natl Acad Sci USA 94:8795–8800.

Springer TA. 1990. Adhesion receptors of the immune system. Nature 346: 425–434.

Springer TA. 1994. Traffic signals for lymphocyte recirculation and leukocyte emigration: The multistep paradigm. Cell 76:301–314.

Taner SB, Onfelt B, Pirinen NJ, McCann FE, Magee AI, Davis DM. 2004. Control of immune responses by trafficking cell surface proteins, vesicles and lipid rafts to and from the immunological synapse. Traffic 5: 651–661.

Varma R, Campi G, Yokosuka T, Saito T, Dustin ML. 2006. T cell receptor-proximal signals are sustained in peripheral microclusters and terminated in the central supramolecular activation cluster. Immunity 25: 117–127.

Walseng E, Bakke O, Roche PA. 2008. Major histocompatibility complex class II–peptide complexes internalize using a clathrin- and dynamin-independent endocytosis pathway. J Biol Chem 283:14717–14727.

Wulfing C, Davis MM. 1998. A receptor/cytoskeletal movement triggered by costimulation during T cell activation. Science 282:2266–2269.

Wulfing C, Sjaastad MD, Davis MM. 1998. Visualizing the dynamics of T cell activation: intracellular adhesion molecule 1 migrates rapidly to the T cell/B cell interface and acts to sustain calcium levels. Proc Natl Acad Sci USA 95:6302–6307.

Yokosuka T, Sakata-Sogawa K, Kobayashi W, Hiroshima M, Hashimoto-Tane A, Tokunaga M, Dustin ML, Saito T. 2005. Newly generated T cell receptor microclusters initiate and sustain T cell activation by recruitment of Zap70 and SLP-76. Nat Immunol 6:1253–1262.